

Hydrosilylation and Silane Polymerization Catalyzed by Group 4 Amidometalocene Cations

Tereza Edlová, Adrien T. Normand,* Hélène Cattey, Stéphane Brandès, Yue Wu, Ariana Antonangelo, Benjamin Théron, Quentin Bonnin, Mariolino Carta, and Pierre Le Gendre*



Cite This: <https://doi.org/10.1021/acs.organomet.2c00642>



Read Online

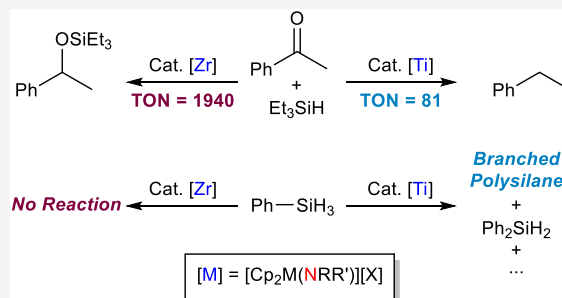
ACCESS |

Metrics & More

Article Recommendations

Supporting Information

ABSTRACT: Four cationic amidotitanocene complexes $[\text{Cp}_2\text{Ti}(\text{NRR}')][\text{B}(\text{C}_6\text{F}_5)_4]$ ($\text{Cp} = \eta^5\text{-C}_5\text{H}_5$; **1a**: $\text{R} = \text{R}' = p\text{-anisyl}$; **1b**: $\text{R} = p\text{-fluorophenyl}$, $\text{R}' = p\text{-anisyl}$; **1c**: $\text{R} = p\text{-fluorophenyl}$, $\text{R}' = \text{phenyl}$; **1d**: $\text{R} = \text{phenyl}$, $\text{R}' = 2\text{-pyridyl}$) were synthesized. Complexes **1a–d** undergo Ti–N bond homolysis under visible light irradiation. Complexes **1a–c** catalyze the polymerization of phenylsilane to yield branched polysilane polymers with molecular weights (M_w) up to approximately 3000 and dispersity indexes (\mathcal{D}) of 1.4–1.6. Previously reported Group 4 cationic amidometalocene complexes $[\text{Cp}_2\text{Ti}(\text{NPh}_2)][\text{B}(\text{C}_6\text{F}_5)_4]$ (**Ia**) and $\text{Cp}_2\text{Zr}(\text{NPh}_2)[\text{MeB}(\text{C}_6\text{F}_5)_3]$ (**IIa**) were also tested in the hydrosilylation of carbonyl compounds with triethylsilane (Et_3SiH). In some cases, complex **Ia** afforded completely reduced products (e.g., ethylbenzene from acetophenone), while **IIa** was generally more selective (e.g., (1-phenylethoxy)-triethylsilane from acetophenone) but also more active. Complex **IIa** could also convert anisole derivatives to phenoxysilanes with high efficiency (TON = 2000).



INTRODUCTION

Group 4 metallocene cations Cp_2MX^+ ($\text{Cp} = \eta^5\text{-C}_5\text{H}_5$, $\text{X} = \text{alkyl}$) are an important class of olefin polymerization catalysts, due to their electrophilicity and coordinatively unsaturated nature.^{1,2} However, they are generally too reactive to be isolated and are thus prepared by the *in situ* reaction of $\text{Cp}_2\text{MX}'_2$ precursors ($\text{X}' = \text{Cl}$ or alkyl) with a cocatalyst (e.g., methylaluminoxane, perfluoroaryl boranes, ammonium salts, etc.).^{3,4}

For a number of years, we have been investigating the chemistry of Group 4 $\text{Cp}_2\text{M}(\text{ERR}')^+$ cations, where E is a group 15 element.^{5–9} In the case of amidometalocene cations (E = N, Chart 1), the spatial proximity of the nitrogen lone pair of

These complexes efficiently catalyze the hydrogenation of olefins and alkynes under very mild conditions (room temperature, pressure ≤ 2.5 bar), and DFT calculations showed that **Ia–c** act as precatalysts for the extremely reactive Cp_2TiH^+ cation.⁹ A similar mechanism was postulated for **IIa,b**, although in this case the fate of the protonated amide remains unclear (Scheme 1).¹⁰

Scheme 1. Precatalyst Activation with H_2

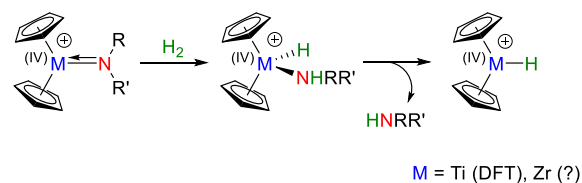
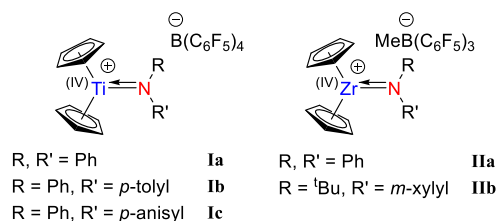


Chart 1. Cationic Group 4 Amidometalocene Complexes



electrons with the d^0 metal center provides sufficient stabilization to make these species “bottlable”: thus, $[\text{Cp}_2\text{M}(\text{NRR}')][\text{X}]$ complexes ($\text{X} = \text{weakly coordinating borate}$; **I**: $\text{M} = \text{Ti}$; **II**: $\text{M} = \text{Zr}$) can be stored indefinitely in the freezer of an Ar glovebox.^{5,9}

Many Ti-catalyzed reactions are thought to proceed via Cp_2TiH , starting from easily accessible Cp_2TiX_2 precatalysts ($\text{X} = \text{F}, \text{Cl}, \text{Me}$), for instance, the dehydrocoupling of ammonia and phosphines with silanes,^{11,12} or that of amine-borane

Special Issue: Early Transition Metals in Organometallic Chemistry

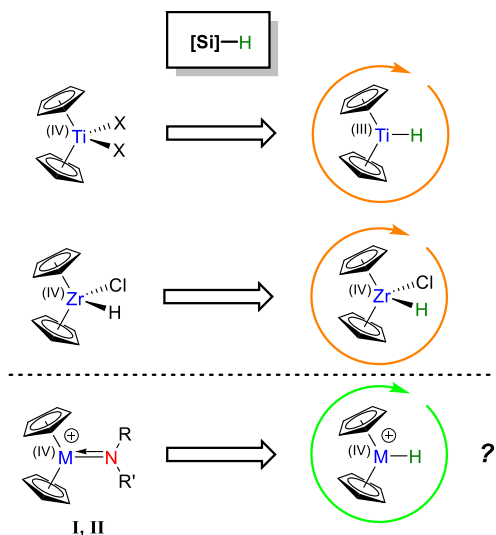
Received: December 22, 2022

adducts;^{13–15} the hydrosilylation of imines and carbonyl compounds;^{16–20} the hydrogenation of imines;^{21,22} the allylation of aldehydes;²³ the deuteriosilylation of epoxides (via Cp₂TiD);²⁴ or the reductive dimerization of amides.²⁵ While versatile, the Cp₂TiH/D manifold (**d**¹, **neutral**) is rather sluggish. As a result, high loadings of Ti (1–10 mol %) and/or forcing conditions are usually required in order to reach acceptable conversions, thus negating the benefits of using an earth-abundant metal.^{26–29}

By contrast with the prevalence of d¹ hydrides observed in Ti chemistry (especially in the metallocene series), the chemistry of Zr hydrides is dominated by Cp₂ZrHCl (a.k.a. Schwartz's reagent, **d**⁰, **neutral**).^{30,31} This complex has largely been used as a stoichiometric reagent for hydrozirconation,^{32,33} although recent reports have shown that catalytic reactions could be developed via the use of silanes to regenerate Cp₂ZrHCl.^{34,35} However, these transformations suffer from the same drawbacks as those catalyzed by Cp₂TiH.

In light of the above, we became interested in exploring the behavior of cationic amidometallocene complexes in catalytic reactions involving silanes, with the hope of gaining access to more efficient Cp₂MH⁺ manifolds (**d**⁰, **cationic**)(Chart 2).

Chart 2. Group 4 Metallocene Hydride Catalytic Manifolds



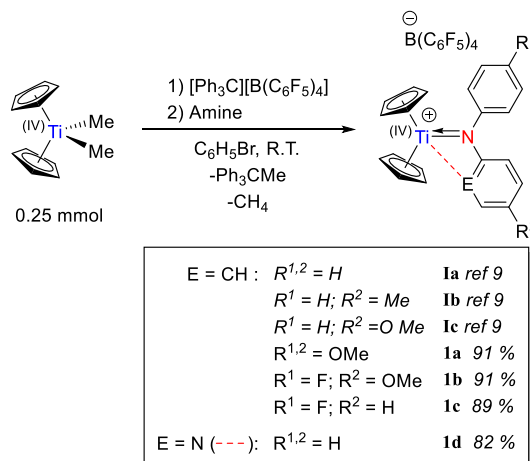
Within this context, it is worth mentioning that complexes **I** also catalyze the dehydrocoupling of amines and silanes with unprecedented turnover numbers (TON approaching 4000) for a nonprecious metal.⁹ Although the mechanism of this transformation has yet to be established, the high activity of **Ia–c** strongly suggests that it does not involve Cp₂TiH as the active catalyst.

In this contribution, we report new cationic amidotitanocene complexes and show that they act as efficient initiators for the polymerization of phenylsilane. Additionally, we report the results of our investigations on the hydrosilylation of aromatic substrates catalyzed by **Ia** and **IIa** and show that high efficiencies (TON up to 2000) can indeed be reached, under mild conditions, for some substrate/catalyst combinations.

RESULTS AND DISCUSSION

Synthesis of New Cationic Amidotitanocene Complexes. Complexes **1a–d** were synthesized in high yields using

Scheme 2. Synthesis of **1a–d**



the same methodology as previously reported, i.e., by aminolysis of Cp₂TiMe⁺ generated *in situ* (Scheme 2).⁹ Compared to previous examples of **I** which contained only H or an electron-donating substituent (Me, OMe) on the *para* position of one of the phenyl rings, complexes **1a–d** span a wider range of electronic properties: from electron-rich (**1a**: OMe, OMe) to push–pull (**1b**: OMe, F) to electron-poor (**1c**: F), and from coordinatively unsaturated (**1a–c**) to saturated (**1d**: pyridine ring). The latter feature has dramatic consequences on the spectroscopic and catalytic properties of **1d**, *vide infra*.

Complex **1d** was characterized by single crystal X-ray diffraction (XRD) analysis, which revealed (as expected) a κ²-N,N' coordination mode for the amide (Figure 1).

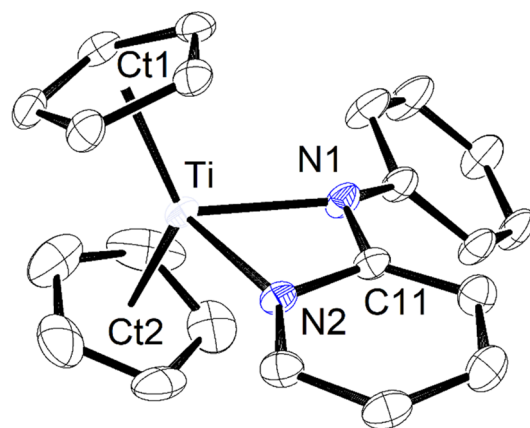


Figure 1. Ortep depiction of the cationic part of **1d**. Ellipsoids drawn at the 50% probability level, Hydrogen atoms omitted for clarity. Relevant bond distances (Å) and angles (deg): Ti–N1: 2.0660(15); Ti–N2: 2.1123(14); Ti–Ct1: 2.0349(9); Ti–Ct2: 2.0291(10); N1–Ti–N2: 64.04(5); Ct1–Ti–Ct2: 134.52(5); C11–N1–Ti–Ct1: 98.88(10).

Surprisingly, the Ti–N1 distance (amide) is only slightly shorter (0.046 Å) than the Ti–N2 distance (pyridine); it is also considerably longer (0.087 Å) than the Ti–N1 distance in **1b**, which was previously characterized by XRD.⁹ Together, these observations indicate that the additional electron donation from the pyridine ring weakens the interaction between the metal and the amide. Moreover, the lone pair of

N1 is almost parallel to the Ti–Ct1 bond, which prevents the development of π interactions with titanium.³⁶ It is also worth noting that N1 is slightly pyramidalized ($\Sigma\alpha(\text{N1}) = 354.0(2)^\circ$), whereas it is perfectly trigonal planar in **1b** ($\Sigma\alpha(\text{N1}) = 360.0(3)^\circ$).

Complexes **1a–d** were characterized by multinuclear NMR, IR, and UV–vis spectroscopies.³⁷ Table 1 gathers relevant

Table 1. Relevant ^1H and ^{15}N NMR Parameters for **1a–d**^a

	Cp	<i>o</i> -Ar ¹	<i>o</i> -Ar ²	N ^b
1a	6.14	5.75		–35
1b	6.11	5.55	5.54	–33
1c	6.14	5.46	5.50	–30
1a	6.31	5.23		–20
1b	6.23	5.47	5.51	–27
1c	6.10	5.84	5.93	–26
1d	6.11	6.40–6.36		–201

^aValues in ppm (values in *italic* taken from ref 9); spectra recorded in C₆D₃Br at 298 K at 600 MHz. ^bAmide signal from $^1\text{H}/^{15}\text{N}$ HMBC experiments.

NMR parameters, along with previously published data for **1a–c**. The shielding of *ortho* Hs of the aryl rings observed in the ^1H NMR spectra of **1a–c** (5.46–5.75 ppm) is retained in **1a–c** (5.23–5.93 ppm), as a consequence of coordinative unsaturation.⁹ By contrast, the *ortho* Hs of the phenyl ring of **1d** resonate at much lower field (~ 6.38 ppm). In addition, the ^{15}N NMR signal of N1 in **1d** is much more shielded (–201 ppm) compared to other complexes (–20 to –35 ppm), as a consequence of the absence of π donation to Ti.³⁸

The UV–vis spectra of **1a–c** recorded in C₆H₅Br at room temperature are characterized by a strong absorption ($\epsilon = 7000\text{--}9000\text{ M}^{-1}\cdot\text{cm}^{-1}$) in the violet region of the visible spectrum ($\lambda = 398\text{--}428\text{ nm}$). By analogy to the situation in phosphidotitanocene cations, we assign this absorption to a LCMT transition with $\pi\text{--}\pi^*$ character localized at N and Ti (Figure 2).⁸ By contrast, **1d** displays an absorption at a much

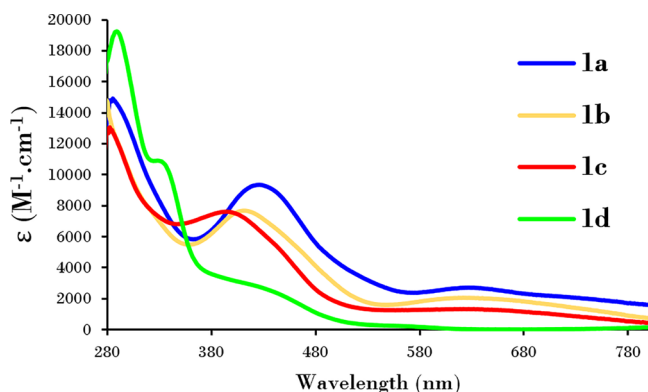
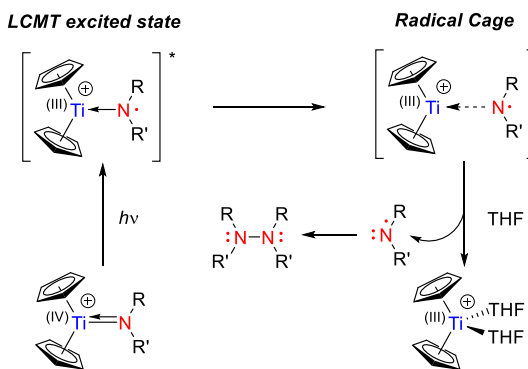


Figure 2. UV–vis spectra of **1a–d** in C₆H₅Br.

higher energy ($\lambda = 333\text{ nm}$), albeit of similar intensity ($\epsilon = 11000\text{ M}^{-1}\cdot\text{cm}^{-1}$).

We have previously shown that amidotitanocene cations readily decompose by Ti–N bond homolysis under visible light irradiation (Scheme 3).⁹ This behavior is typical of LMCT reactivity at a 3d metal,³⁹ and it is exacerbated by the well-documented reducibility of d⁰ titanocene derivatives on the one hand^{40–42} and the strong basicity of amides on the other hand.⁴³ The resulting Ti(III) complex can be trapped in the presence of THF.

Scheme 3. LMCT Reactivity of Amidotitanocene Cations



Irradiation of THF/toluene solutions of **1a–c** (18W LED, 405 or 450 nm) for 10 s indeed led to the formation of $\text{Cp}_2\text{Ti}(\text{THF})_2^+$, which can be observed by EPR spectroscopy ($g = 1.9758$, $A^{47/49\text{Ti}} = 11.4 \times 10^{-4}\text{ cm}^{-1}$),⁸ see Figures S40–S42. For **1d**, more forcing conditions had to be used, i.e., irradiation for 2 h in neat THF-*d*₈ (Figure 3). This behavior is in line with

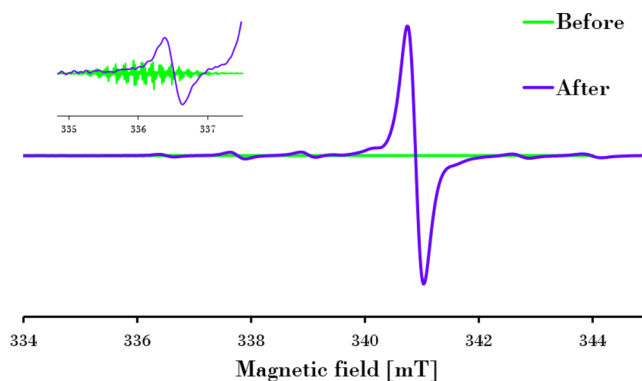


Figure 3. EPR spectra of **1d** in THF-*d*₈ before and after irradiation (18W LED, 450 nm).

the expectation that **1d** should be more stable than its coordinatively unsaturated counterparts.

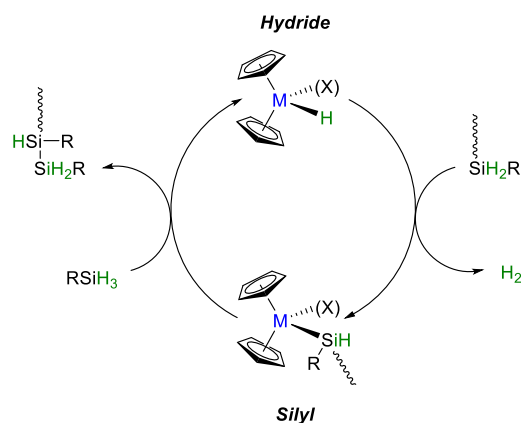
As shown in Figure 3 the solution of **1d** before irradiation already contains minute amounts of a paramagnetic species, which we have not been able to identify. After irradiation, the concentration of this species compared to $\text{Cp}_2\text{Ti}(\text{THF})_2^+$ is negligible (see the expansion in the upper left corner). Similar observations were made for **1a–c** (Figures S9, S18, and S29),⁴⁴ as well as **1a–c**.⁹ As noted previously, these species are probably not aminyl free radicals, because the values of the A^{N} coupling constants ($3.67\text{--}7.17 \times 10^{-4}\text{ cm}^{-1}$) are consistently smaller than those reported in the literature.^{45–47} Rather, we suggest the presence of Ti(IV)-stabilized aminyl radicals: The exact nature of the Ti(IV) fragment remains elusive, but given the simulated spectra, it likely does not contain additional nitrogen atom(s).

Phenylsilane Polymerization. Group 4 metallocene complexes have been studied extensively for the polymerization of primary silanes (RSiH_3).^{48–63} The resulting narrowly dispersed, linear polysilanes possess interesting properties such as high UV absorption, σ -electron delocalization, and photodegradability.^{64–68} Depending on the catalyst, variable amount of cyclic oligomers (RSiH)_n and silane redistribution products (e.g., R_2SiH_2 , R_3SiH) are obtained as side-products.⁶⁹ In general,

Zr catalysts are more active than Ti catalysts, and they are also more selective. However, precatalyst activation plays an important part in the outcome of the reaction. Thus, mixtures of $\text{Cp}_2\text{MCl}_2/2\text{BuLi}/\text{B}(\text{C}_6\text{F}_5)_3$ are clearly more active in the case of Zr ($M_w = 3800$ vs 780 for Ti),⁵³ while for mixtures of $\text{Cp}_2\text{MCl}_2/2\text{MeLi}$ the difference is less flagrant ($M_w = 2296$ vs 1843 for Ti).⁵¹ Nevertheless, longer polymer chains are usually obtained with Zr catalysts (e.g., $M_w = 13880$ g·mol⁻¹ with $[\text{CpCp}^*\text{ZrH}_2]_2$).⁵⁹

Based on stoichiometric studies, Tilley proposed a polymerization mechanism involving a sequence of σ -bond metathesis steps with d⁰ metal hydrides and silyl intermediates (Scheme 4).⁵⁸

Scheme 4. Tilley's Mechanism of Silane Polymerization



However, alternative mechanisms (e.g., involving silylene complexes or silyl free radicals) have been suggested,^{49,70} and while Tilley's mechanism is now largely accepted,⁷¹ it does leave some questions unanswered, such as the charge and the oxidation state of the intermediates (especially in the case of "cation-like" catalysts obtained by activation with *n*BuLi and $\text{B}(\text{C}_6\text{F}_5)_3$).

Complexes **Ia** and **Ia-c** were found to be active catalysts for the polymerization of phenylsilane at room temperature (Table 2). By contrast, **Id** and **Iia** were completely inactive. For **Id**, this result is probably due to the absence of free

coordination site at Ti. On the other hand, the lack of activity of **Iia** was surprising. Harrod has shown that precatalyst activation procedures that generate Cp_2ZrH^+ *in situ* are not conducive to silane polymerization,⁷⁰ which could explain our results. However, as noted by Harrod, these observations are difficult to reconcile with Tilley's mechanism.⁵³

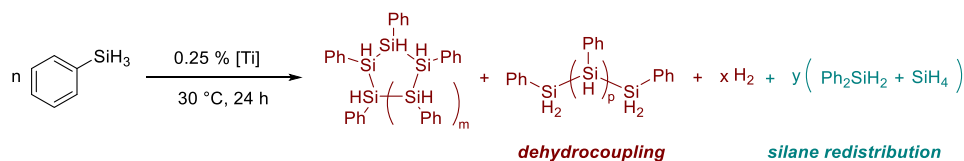
Two fractions, liquid and polymeric, were isolated from the viscous reaction mixture (after dissolution in toluene, followed by polymer precipitation from pentane). As shown in the simplified reaction equation above Table 2, active Ti catalysts also generate important quantities of silane redistribution products (mainly diphenylsilane and SiH_4 gas).

Analysis of the liquid fraction (after solvent evaporation) by ¹H NMR spectroscopy and ²⁹Si DEPT revealed the presence of additional silane redistribution products such as $(\text{Ph}_2\text{SiH})_2$ and Ph_3SiH (Figure S47).^{72,73} Pure diphenylsilane was obtained in 6–21% yield from this mixture following bulb-to-bulb distillation. The rubbery residue after distillation was not analyzed, but weighed to assess the mass balance of the reaction.

Polymer fractions were analyzed by gel-permeation chromatography (GPC). As shown in Table 2, the yield and molecular weight of these fractions show some variability, due to the bulk reaction conditions and workup procedure. Because of this variability, the identification of catalyst-dependent trends is complicated. Interestingly, however, a unimodal distribution ($M_w = 1691$ –3053; \bar{D} : 1.4–1.6) was observed in every case (Figure S53), which indicates that the amount of cyclic oligomers lies below the GPC detection limit.⁷⁴ Titanium catalysts usually yield large amounts of cyclic oligomers, therefore our complexes seem to possess a distinct selectivity. They are also quite active: 23–49 kg(PSi)·mol(Ti)⁻¹·mol(Si)⁻¹·h⁻¹, compared to 0.9 kg(PSi)·mol(Ti)⁻¹·mol(Si)⁻¹·h⁻¹ for $\text{Cp}_2\text{TiCl}_2/2\text{BuLi}$.⁶¹

Polymer **PSi-1** ($M_w = 3053$; $\bar{D} = 1.4$), obtained from run **1b-1**, was characterized by UV-vis, IR, and ¹H and ²⁹Si DEPT NMR spectroscopies.⁷⁵ As a consequence of σ -electron delocalization, this polymer strongly absorbs UV light below 340 nm (Figure S50).⁷⁶

Table 2. Silane Polymerization Results^a



catalyst	run	polymer fraction						liquid fraction				
		polymer yield (mg)	act. ^b	Mn (g mol ⁻¹)	Mw (g mol ⁻¹)	DP ^c	\bar{D}	Ph_2SiH_2 yield (mg)	TON	residue (mg)	material recovery (%)	
Ia	1	729	47	1182	1691	15	1.4	267	36	532	87	
Ia	2	659	42	1274	1782	16	1.4	188	25	588	82	
Ia	1	497	32	1188	1697	15	1.4	587	78	424	86	
Ia	2	359 ^d	23	1619	2489	21	1.5	574	76	576	86	
Ib	1	583	37	2156	3053	27	1.4	626	83	450	94	
Ib	2	518	33	1816	2889	23	1.6	443	59	580	88	
Ic	1	651	42	1898	2883	24	1.5	346	46	548	88	
Ic	2	760 ^e	49	1250	1778	16	1.4	230	31	566	88	

^aSimplified equation; Mn and Mw values estimated using polystyrene calibration. Reagents and conditions: phenylsilane (2 mL, 16.3 mmol), catalyst (0.04 mmol), 30 °C, 24 h. Isolated yield after fractionation and distillation. ^bActivity in kg(PSi)·mol(Ti)⁻¹·mol(Si)⁻¹·h⁻¹. ^cDegree of polymerization estimated according to ref 62. ^dThe product formed a gum which was reprecipitated. ^eThe product formed a gum which was redissolved and evaporated to dryness.

The IR spectrum of **PSi-1** shows a broad and intense band at 2084 cm^{-1} , assigned to stretching vibrations of internal SiH bonds (Figure S51).⁷⁶

The ^1H and ^{29}Si DEPT 90 NMR spectra of **PSi-1** are shown in Figure 4. Broad signals were observed in both cases, along

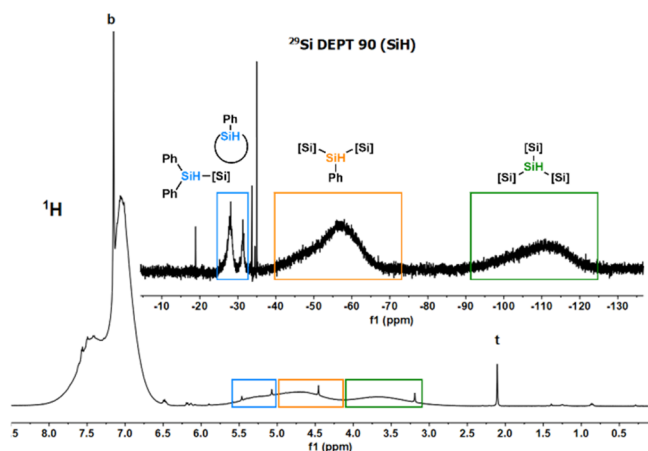


Figure 4. ^1H (bottom) and ^{29}Si DEPT 90 (top) NMR spectra of **PSi-1** (600 and 119 MHz, C_6D_6 , 298 K) (b: benzene signal; t: toluene signal).

with sharp signals due to traces of solvents, linear oligomers, and diphenylsilane.

Three distinct regions are observed in each spectrum:⁷⁷

- Blue regions (^1H : 5.0–5.6 ppm; ^{29}Si : –32 to –25 ppm): these signals are generally assigned to cyclic oligomers. However, given the unimodal distribution observed by GPC, we think that these signals could also be due to $\text{Ph}_2\text{SiH-}$ chain ends. As observed by Waterman, these are likely to originate from the redistribution of PhSiH_2- chain ends.⁷³
- Orange regions (^1H : 4.1–5.0 ppm; ^{29}Si : –70 to –40 ppm): these signals are typical of linear polyphenylsilane samples containing PhSiH- repeat units.⁷⁶ The ^{29}Si DEPT 135 spectrum of **PSi-1** also indicates the presence of PhSiH_2- end groups in this region (Figure S49).
- Green regions (^1H : 3.1–4.0 ppm; ^{29}Si : –125 to –92 ppm). Signals in these regions have previously been assigned to SiH_3 chain ends⁷⁸ or internal SiH_2 repeat units.⁷³ However, in our case, they can only be due to internal SiH branch points;⁷⁹ otherwise, no signal would be observed in the ^{29}Si DEPT 90 spectrum.

Catalytic Hydrosilylation. Group 4 metals have long been known to catalyze the hydrosilylation of carbonyl compounds and imines.^{16–19,21,22,34,35,80–85} In order to explore the potential of group 4 amidometalocene cations in this area, we screened the reaction of aromatic carbonyl compounds with Et_3SiH in the presence of a catalytic amount of **Ia** or **IIa** in $\text{C}_6\text{H}_5\text{Br}$ (Table 3).

By contrast to its lack of activity in the polymerization of phenylsilane, Zr complex **IIa** was consistently more active than **Ia**, and high TONs (up to 2000 in 24 h) could be achieved under mild conditions (30 °C). For instance, benzaldehyde underwent clean hydrosilylation to give the corresponding silanoxy ether in quantitative yield (entry 1). Interestingly, under the same conditions, **Ia** gave instead a complex mixture containing brominated diphenylmethane isomers (entry 2). This result is not entirely unexpected, since Friedel–Crafts

reactions of benzaldehyde with arenes promoted by Lewis or Brønsted acids have previously been reported.^{86,87} Moreover, the Ti-catalyzed complete reduction of carbonyl compounds, including aldehydes, has recently been reported.²⁰ Running the reaction in C_6H_6 instead of $\text{C}_6\text{H}_5\text{Br}$ afforded a less complex mixture: (benzyloxy)triethylsilane and diphenylmethane were obtained in 31% and 28% NMR yields, respectively (entry 3). The presence of large quantities of $(\text{Et}_3\text{Si})_2\text{O}$ was also observed by ^1H NMR spectroscopy and GCMS (Figures S59 and S60), as in all the other reaction mixtures involving carbonyl deoxygenation.

The reaction of acetophenone with Et_3SiH also had contrasting outcomes depending on the catalyst. In the presence of **IIa**, the corresponding silanoxy ether was obtained in almost quantitative yield (entry 4); in the presence of **Ia**, ethylbenzene was obtained instead (entry 5).

Running the reaction with a higher loading of Zr (1.0% instead of 0.05%) gave the same product (entry 6), while reducing the loading of Ti (0.05% instead of 1.0%) suppressed the formation of ethylbenzene (entry 7); therefore, one can reasonably assume that (1-phenylethoxy)triethylsilane is an intermediate along the path to the complete reduction of acetophenone.

Methyl benzoate could also be hydrosilylated in the presence of **IIa**, to give (benzyloxy)triethylsilane in 81% yield (entry 8). A small amount (13%) of silanoxy hemiacetal was also observed (along with MeOSiEt_3 , see Figures S69 and S70). Increasing the temperature and reaction time (entry 9; 40 °C, 72 h) resulted in a slightly higher product ratio in favor of (benzyloxy)triethylsilane (93/7). This result suggests that the silanoxy mixed acetal could be an intermediate along the path to the partial reduction of methyl benzoate. In the presence of **Ia** (entry 10), a complex mixture was observed, in which (benzyloxy)triethylsilane (38%) and toluene (11%) were observed, along with brominated diphenylmethane isomers (Figures S73 and S74).

Benzoic acid could be reduced in the presence of **IIa** (entries 11 and 12), but not in the presence of **Ia** (entry 13). In the former case, complete conversion to a mixture of (benzyloxy)triethylsilane and benzaldehyde(triethylsilyl)acetal was observed.⁸⁸ Interestingly, increasing the reaction temperature from 30 °C (entry 11) to 40 °C (entry 12) hardly changed the ratio between both products, which suggests that catalyst deactivation could occur.

The results described above indicate that, depending on the combination of catalyst/substrate, different mechanisms may operate. In fact, even precatalyst activation is likely to follow different pathways for Ti and Zr, although in each case Cp_2MH^+ species are postulated:

- For Ti, we have shown previously that amidotitanocene cations react with Et_3SiH to form the corresponding (amino)silane and a mixture of paramagnetic species resulting from the decomposition of Cp_2TiH^+ (Scheme 5, top).⁹
- By contrast, Zr complex **IIa** does not react with Et_3SiH ; however, addition of PhCHO immediately leads to the formation of (benzyloxy)triethylsilane (Figure S95). Furthermore, we also observed the reaction of **IIa** with PhCHO to yield **IIIa**, following aldehyde insertion into the Zr–N bond.⁵ This reactivity suggests that the activation of amidozirconocene precatalysts could proceed similarly with nonenolizable carbonyl compounds (Scheme 5, middle). For substrates containing

Table 3. Reaction of Aromatic Substrates with Et₃SiH

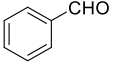
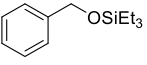
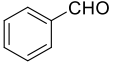
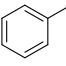
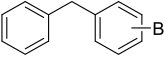
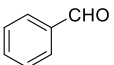
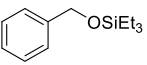
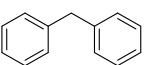
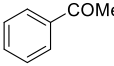
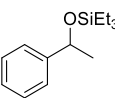
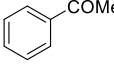
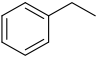
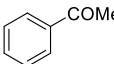
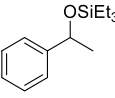
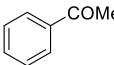
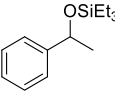
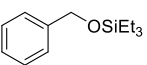
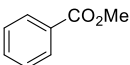
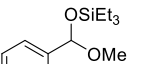
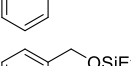
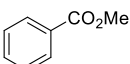
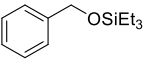
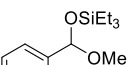
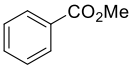
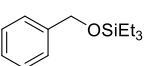
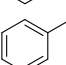
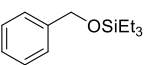
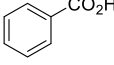
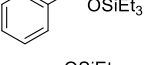
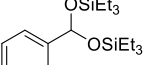
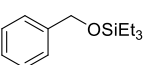
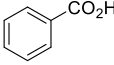
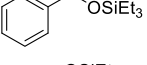
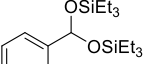
Entry	Substrate	Silane eq.	M	Loading (mol%)	Conv. (%)	Product(s)	Mechanism ^[a]	NMR Yield (%)
1		2.0	Zr	0.05	100		(2)	100
2		3.0	Ti	1.0	100	 	(2)-(3)-(4)-(6)	8/N/A ^[b]
3		3.0	Ti	1.0	100	 	(2)-(3)-(6)	31/28 ^{[b],[c]}
4		2.0	Zr	0.05	100		(2)	97
5		2.0	Ti	1.0	100		(2)-(4)-(6)	81
6		2.0	Zr	1.0	100		(2)	92
7		2.0	Ti	0.05	25	 	(2)-(4)-(6)	14
8		3.0	Zr	0.05	100	 	(2)-(5)	81/13
9		3.0	Zr	0.05	100	 	(2)-(5)	93/7 ^{[d],[e]}
10		4.0	Ti	1.0	100	  	(2)-(5)-(6)-(7)	38/11 ^{[b],[d]}
11		4.0	Zr	0.5	100	  	(1)-(2)-(5)	25/76 ^[d]
12		4.0	Zr	0.5	100	 	(1)-(2)-(5)	20/83 ^{[d],[e]}

Table 3. continued

Entry	Substrate	Silane eq.	M	Loading (mol%)	Conv. (%)	Product(s)	Mechanism ^[a]	NMR Yield (%)
13		4.0	Ti	1.0	8	N/A	N/A	N/A ^[d]
14		3.0	Zr	1.0	1	N/A	N/A	N/A ^{[d],[f]}
15		3.0	Zr	0.5	100		(2)-like	88 ^[d]
16		2.0	Zr	0.05	100		Scheme 7	100
17		2.0	Ti	1.0	8		Scheme 7	8
18		3.0	Zr	0.05	100		Scheme 7	100
19		4.0	Zr	1.0	15	N/A	N/A	N/A ^{[d],[f]}
20		4.0	Zr	1.0	14	N/A ^[g]	N/A	N/A ^{[d],[f]}

^aRefer to Scheme 6. Reagents and conditions: substrate (1.00 mmol), silane, catalyst, C₆H₅Br (1.0 mL), 30 °C, 24 h. Conversion and NMR yields were estimated by ¹H NMR spectroscopy (average of two runs). ^bUnquantified presence of isomeric Friedel–Crafts products. ^cIn C₆H₆. ^d72 h. ^e40 °C. ^f60 °C. ^g(Et₃Si)₂O (13%) was observed by ¹H NMR and GCMS.

acidic hydrogens (i.e., ketones and carboxylic acid), protonation of the amido ligand, to form Zr-carboxylates and Zr enolates, respectively, also appears feasible (Scheme 5, bottom).

Following precatalyst activation, we propose the mechanisms delineated in Scheme 6:

- eq (1): A carboxylic acid undergoes dehydrocoupling to yield a silanoxo ester. A similar mechanism can be envisaged for the formation of silanoxo ethers from phenols (not shown). This step appears to be specific to Zr.
- eq (2): A carbonyl compound (i.e., aldehyde, ketone, ester) undergoes hydrometalation to yield a group 4 alcoholate. From this intermediate, Cp₂MH⁺ can be regenerated to liberate a silanoxo ether or mixed acetal.
- eq (3): In the case of aldehydes, the Ti alcoholate can also undergo an S_EAr with the aromatic solvent, to yield an arenium cation and Cp₂Ti=O. The oxo complex deprotonates the arenium cation to yield the Friedel–Crafts product, and following dehydrocoupling of the protonated oxo complex with Et₃SiH, a Ti silanoxylate (Cp₂TiOSiEt₃⁺) is generated.
- eq (4): A silanoxo ether generated in eq (2) undergoes deoxygenation by Cp₂TiH⁺ to yield an alkane and Cp₂TiOSiEt₃⁺.
- eq (5): A silanoxo (mixed) acetal generated in eq (2) undergoes partial deoxygenation to yield (benzyloxy)-triethylsilane and a group 4 alcoholate or silanoxylate (Cp₂MOR⁺).
- eq (6): Cp₂MH⁺ is regenerated from Cp₂MOR⁺, yielding a silanoxo ether.

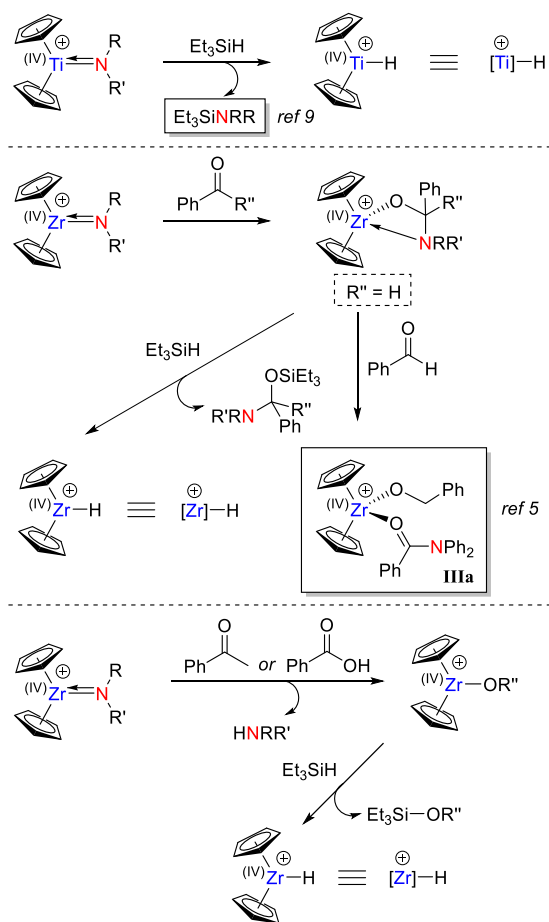
- eq (7): Et₃SiOMe generated in eq (6) reacts further with Cp₂TiH⁺ to yield methane and (Et₃Si)₂O. This step appears to be specific to Ti.⁸⁹

Finally, in addition to carbonyl compounds, benzonitrile and anisole derivatives reacted with Et₃SiH in the presence of **IIa**, to give *N*-(triethylsilyl)benzaldehyde imine and (aryloxy)-triethylsilanes, respectively (entries 15–18). In the case of anisole derivatives, the high activity of **IIa** is interesting in the context of protecting group interconversion (i.e., from methoxy to silyloxy).^{90,91} From a mechanistic point of view, stoichiometric experiments indicate that **IIa** only engages in coordination/dissociation equilibria with Et₃SiH and anisole: Only when both reagents are present does the silylation proceed (Figure S96). Thus, this transformation probably proceeds via a Zr-activated silane (Scheme 7).^{90,92} Finally, **IIa** failed to catalyze the reaction of Et₃SiH with the following compounds: *N,N*-dimethylbenzamide (entry 14), *p*-anisidine (entry 19), and nitrobenzene (entry 20).

CONCLUSION

We have reported novel examples of cationic amidotitanocene complexes (**1a–d**). In the case of pyridyl derivative **1d**, the saturation of the coordination sphere of Ti results in the loss of Ti=N double-bond character. Complex **1d** was completely inactive in the polymerization of phenylsilane, whereas **1a–c** and parent amidotitanocene complex **1a** led to branched polysilanes with increased activities (up to 50-fold) compared to the Cp₂TiCl₂/2BuLi system. Remarkably, parent amidotitanocene complex **IIa** was completely inactive in this transformation, in contrast with the usual behavior of Zr catalysts. On the other hand, **IIa** gave exceptional results in the reaction of carbonyl compounds and anisole derivatives with Et₃SiH

Scheme 5. Proposed Mechanisms for Precatalyst Activation in the Reaction of Carbonyl Compounds with Et₃SiH^a



^aAnions are omitted for clarity.

(TONs up to 2000 at 30 °C), which bode well for future applications in protecting groups interconversion or depolymerization processes (e.g., of polyesters). While **1a** was found to be less active in these transformations, it also displayed complementary selectivity and was able to reduce carbonyl compounds all the way to alkanes. Experimental evidence thus indicates that Ti and Zr catalysts probably operate according to distinct mechanisms, including during precatalyst activation.

The view of group 4 amidometallocene cations as Cp₂MH⁺ precursors is somewhat reductive: For instance, the reactivity of anisole derivatives suggests that **IIa** simply acts as a strong Lewis acid to activate the silane. In depth mechanistic studies are undoubtedly warranted in order to fully unlock the potential of these species, which continue to demonstrate impressive catalytic performances for an increasing number of transformations that are relevant to current industrial challenges.

EXPERIMENTAL SECTION

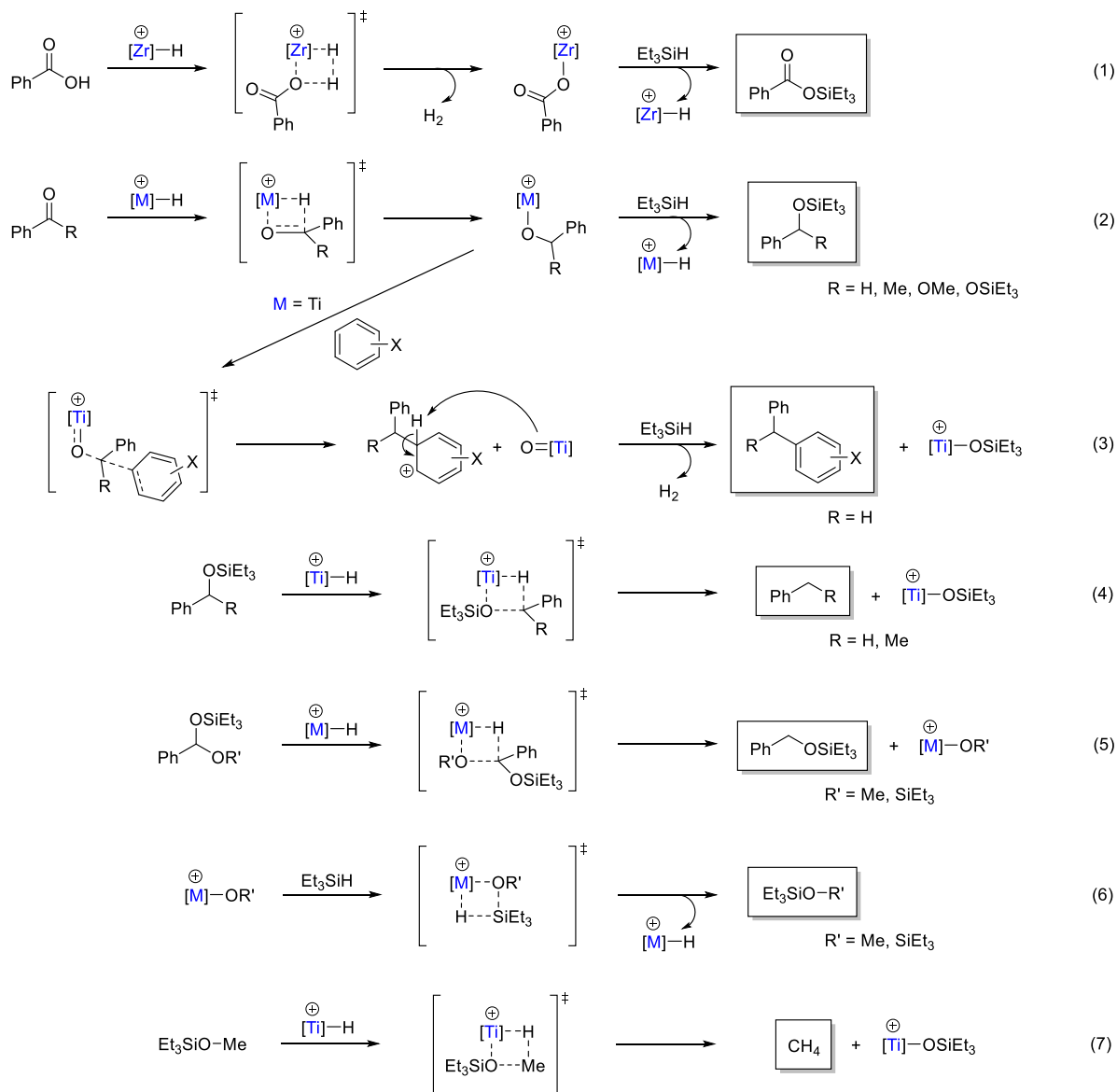
General Considerations. All reactions were carried out under Ar using conventional Schlenk techniques or in an Ar glovebox. Toluene, CH₂Cl₂, Et₂O, pentane, and THF were dried using an MBraun MB SPS-800 solvent purification system. Bromobenzene was distilled over CaH₂ and stored over activated 3 Å molecular sieves in the glovebox. Deuterated solvents and Et₃SiH were dried by passage through a short column of activated neutral alumina (Brockman grade II) and stored over activated 3 Å molecular sieves in the glovebox, either at room temperature (C₆D₆, C₆D₃Br, ...) or at -18 °C (THF-*d*₈, CD₂Cl₂,

Et₃SiH). Alumina and molecular sieves were activated by heating for at least 6 h above 230 °C under vacuum. Diatomaceous earth (dicalite) was dried in an oven at 110 °C. The following compounds were prepared according to literature procedures: [Cp₂TiMe₂],⁹³ [Ph₃C][B(C₆F₅)₄] (from Ph₃CCl and [Li(OEt)_{2.5}][B(C₆F₅)₄]),⁹⁴ 4-fluoro-*N*-(4-methoxyphenyl)aniline,⁹⁵ 4-fluoro-*N*-phenylaniline,⁹⁵ and *N*-phenylpyridin-2-amine.⁹⁶ All other reagents were used as received from chemical suppliers.

Synthesis of Compounds. Complexes **1a–d** were prepared on a 0.25 mmol scale using the previously reported procedure.⁹ In an Ar glovebox, three solutions were prepared, each containing 1 equiv of reagent in C₆H₅Br: Solution A (freshly prepared [Cp₂TiMe₂], 0.3 mL), Solution B ([Ph₃C][B(C₆F₅)₄], 0.3 mL), and Solution C (amine, 0.3 mL). Solution A was stirred magnetically and solutions B, then C, were added dropwise with a pipet. The effervescent reaction mixture was stirred for 5 min, before being added to 50 mL of pentane under vigorous agitation. The precipitated solid was filtered over a sintered glass frit and dried in the glovebox. Complexes **1a–c** were obtained as dark green powders, and complex **1d** was obtained as a bright red powder.

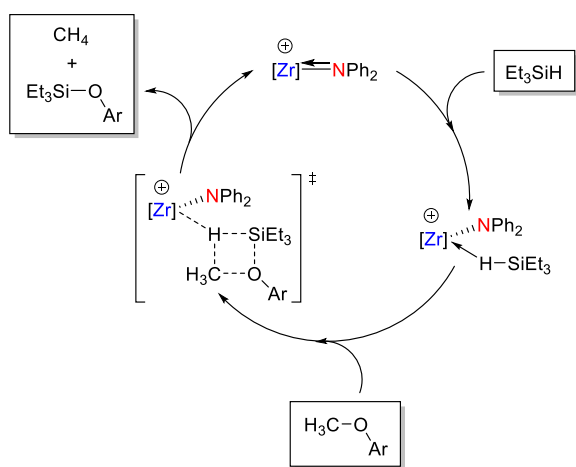
Complex 1a. Prepared according to the general procedure starting from dimethyltitanocene (0.0520 g, 0.25 mmol), trityl tetrakis(pentafluorophenyl)borate (0.2320 g, 0.25 mmol), and 4,4'-dimethoxydiphenylamine (0.0573 g, 0.25 mmol). The workup afforded the product as a dark green powder containing 1.2 equiv of pentane (268 mg, 91%). Elemental Analysis: % Calcd for C₄₈H₂₄BF₂₀NO₂Ti: C, 53.12; H, 2.23; N, 1.29. Found: C, 53.93; H, N.D.; N, 1.73. UV-vis (C₆H₅Br, 0.1 mm cell): λ_{max} = 428 nm (9300 M⁻¹·cm⁻¹). IR (ATR): 3117 (b, w), 2933 (w), 2922 (w), 2842 (w), 1642 (m), 1586 (m), 1511 (s), 1470 (m), 1455 (s), 1373 (w), 1358 (w), 1299 (w), 1274 (m), 1246 (m), 1182 (w), 1164 (w), 1080 (s), 1028 (m), 973 (s), 820 (s), 768 (m), 755 (s), 726 (w), 682 (m), 660 (m), 601 (w), 572 (w). ¹H NMR (600 MHz, 298 K, C₆D₃Br): δ = 6.68 (m, 4H, *m* of NAr), 6.31 (s, 10H, Cp), 5.23 (m, 4H *o* of NAr), 3.55 (s, 6H, OCH₃). ¹³C{¹H} NMR (151 MHz, 298 K, C₆D₃Br): δ = 161.1 (s, *p* of NAr), 148.5 (dm, ¹J_{CF} = 240 Hz, *o* of C₆F₅), 147.2 (s, *i* of NAr), 138.3 (dm, ¹J_{CF} = 240 Hz, *p* of C₆F₅), 136.5 (dm, ¹J_{CF} = 240 Hz, *m* of C₆F₅), 124.4 (bs, BC), 123.4 (s, Cp), 119.3 (s, *o* of NPh), 115.8 (s, *m* of NAr), 55.3 (s, CH₃). ¹⁹F{¹H} NMR (194 MHz, 298 K, C₆D₃Br): δ = -16.2. ¹⁹F{¹H} NMR (565 MHz, 298 K, C₆D₃Br): δ = -131.7 (br s, 8F, *o* of C₆F₅), -161.6 (m, 4F, *p* of C₆F₅), -165.5 (br s, 8F, *m* of C₆F₅).

Complex 1b. Prepared according to the general procedure starting from dimethyltitanocene (0.0520 g, 0.25 mmol), trityl tetrakis(pentafluorophenyl)borate (0.2320 g, 0.25 mmol), and 4-fluoro-*N*-(4-methoxyphenyl)aniline (0.0543 g, 0.25 mmol). The workup afforded the product as green powder containing 1.7 equiv of pentane and about 4 mol % (by NMR) of Ph₃Et as an impurity (273 mg, 91%). Elemental Analysis: % Calcd for C₄₇H₂₁BF₂₁NO₂Ti: C, 52.59; H, 1.97; N, 1.30. Found: C, 54.85; H, N.D.; N, 2.23. UV-vis (C₆H₅Br, 0.1 mm cell): λ_{max} = 414 nm (7600 M⁻¹·cm⁻¹). IR (ATR): 3105 (b, w), 2960 (w), 2927 (w), 2873 (w), 1641 (m), 1586 (m), 1511 (m), 1492 (m), 1456 (s), 1374 (m), 1283 (w), 1272 (m), 1252 (m), 1226 (m), 1195 (w), 1152 (w), 1082 (s), 1022 (m), 972 (s), 841 (w), 822 (s), 793 (w), 773 (m), 755 (m), 726 (w), 683 (m), 660 (m), 595 (w), 573 (w), 516 (w), 450 (w). ¹H NMR (600 MHz, 298 K, C₆D₃Br): δ = 6.79 (m, 2H, *m* of NC₆H₃F), 6.71 (m, 2H, *m* of NAn), 6.23 (s, 10H, Cp), 5.51 (m, 2H, *o* of NAn), 5.47 (m, 2H, *o* of NC₆H₃F), 3.55 (s, 3H, OCH₃). ¹³C{¹H} NMR (151 MHz, 298 K, C₆D₃Br): δ = 161.7 (d, ¹J_{CF} = 250 Hz, *p* of NC₆H₃F), 161.5 (s, *p* of NAn), 152.7 (s, *i* of NC₆H₃F), 148.5 (dm, ¹J_{CF} = 240 Hz, *o* of C₆F₅), 147.8 (s, *i* of NAn), 138.4 (dm, ¹J_{CF} = 240 Hz, *p* of C₆F₅), 136.6 (dm, ¹J_{CF} = 240 Hz, *m* of C₆F₅), 124.4 (bs, BC), 122.9 (s, Cp), 121.9 (d, ²J_{CF} = 5 Hz, *o* of NC₆H₃F), 117.5 (s, *m* of NAn), 117.3 (s, *o* of NAn), 116.4 (d, ³J_{CF} = 23 Hz, *m* of NC₆H₃F), 55.5 (s, CH₃). ¹⁹F{¹H} NMR (194 MHz, 298 K, C₆D₃Br): δ = -16.2. ¹⁹F{¹H} NMR (565 MHz, 298 K, C₆D₃Br): δ = -112.3 (s, 1F, NC₆H₃F), -131.7 (br s, 8F, *o* of C₆F₅), -161.6 (m, 4F, *p* of C₆F₅), -165.6 (br s, 8F, *m* of C₆F₅).

Scheme 6. Proposed Mechanisms for the Reaction of Carbonyl Compounds with Et₃SiH^{4†}

[†]Framed products have been observed by ¹H NMR spectroscopy and/or GCMS.

Scheme 7. Proposed Mechanism for the Zr-Catalyzed Silylation of Anisole Derivatives



Complex 1c. Prepared according to the general procedure starting from dimethyltitanocene (0.0526 g, 0.25 mmol), trityl tetrakis(pentafluorophenyl)borate (0.2340 g, 0.25 mmol), and 4-fluoro-*N*-phenylaniline (0.0474 g, 0.25 mmol). The workup afforded the product as dark green powder containing 0.1 equiv of pentane (251 mg, 89%). Elemental Analysis: % Calcd for C₄₆H₁₉BF₂₁NTi: C, 52.96; H, 1.84; N, 1.34. Found: C, 52.61; H, N.D.; N, 1.26. UV-vis (C₆H₅Br, 0.1 mm cell): λ_{max} = 398 nm (shoulder, 7700 M⁻¹·cm⁻¹). IR (ATR): 3115 (br, w), 1641 (w), 1596 (w), 1511 (m), 1469 (w), 1456 (s), 1370 (w), 1274 (w), 1229 (w), 1154 (w), 1113 (w), 1084 (s), 985 (w), 972 (s), 887 (w), 834 (w), 821 (m), 769 (m), 753 (m), 698 (w), 683 (m), 662 (m), 630 (w), 610 (w), 601 (w), 573 (w), 546 (w), 538 (w), 518 (w). ¹H NMR (600 MHz, 298 K, C₆D₅Br): δ = 7.16 (m, 2H, *m* of NPh), 7.04–7.00 (m, 1H, *p* of NPh, overlapping with bromobenzene signal), 6.80 (m, 2H, *o* of NAr), 6.10 (s, 10H, Cp), 5.93 (m, 2H, *o* of NPh), 5.84 (m, 2H, *o* of NAr). ¹³C{¹H} NMR (151 MHz, 298 K, C₆D₅Br): δ = 161.3 (d, ¹J_{CF} = 249.8 Hz, *p* of NAr), 158.1 (s, *i* of NPh), 154.9 (s, *i* of NAr), 148.6 (dm, ¹J_{CF} = 240 Hz, *o* of C₆F₅), 138.4 (dm, ¹J_{CF} = 240 Hz, *p* of C₆F₅), 136.6 (dm, ¹J_{CF} = 240 Hz, *m* of C₆F₅), 131.6 (s, *m* of NPh), 129.0 (s, *p* of NPh), 124.5 (bs, BC), 122.1 (d, ³J_{CF} = 8.1 Hz, *o* of NAr),

121.8 (s, Cp), 117.9 (s, *o* of NPh), 116.7 (d, $^2J_{CF} = 22.7$ Hz, *m* of NAr). $^{11}B\{^1H\}$ NMR (194 MHz, 298 K, C_6D_5Br): $\delta = -16.1$. $^{19}F\{^1H\}$ NMR (565 MHz, 298 K, C_6D_5Br): $\delta = -112.1$ (s, 1F, NAr)–131.7 (bs, 8F, *o* of C_6F_5), –161.6 (m, 4F, *p* of C_6F_5), –165.6 (br s, 8F, *m* of C_6F_5).

Complex 1d. Prepared according to the general procedure starting from dimethyltitanocene (0.0520 g, 0.25 mmol), trityl tetrakis(pentafluorophenyl)borate (0.2320 g, 0.25 mmol), and *N*-phenylpyridin-2-amine (0.0426 g, 0.25 mmol). The workup afforded the product as orange-red powder (226 mg, 82%) containing residual pentane (about 0.3 equiv). Single crystals suitable for X-ray diffraction were obtained by diffusion of cyclohexane into a chlorobenzene solution of **1d** at ambient temperature. Elemental Analysis: % Calcd for $C_{45}H_{19}BF_{20}N_2Ti$: C, 52.66; H, 1.87; N, 2.73. Found: C, 52.70; H, N.D.; N, 2.79. UV–vis (C_6H_5Br , 0.1 mm cell): $\lambda_{max} = 432$ nm (shoulder, $2600 M^{-1}cm^{-1}$), 333 nm ($10\ 800 M^{-1}cm^{-1}$). IR (ATR): 3120 (br, w), 1602 (w), 1600 (w), 1510 (m), 1449 (s), 1366 (m), 1272 (m), 1215 (w), 1158 (w), 1081 (m), 997 (w), 972 (s), 833 (s), 769 (m), 754 (s), 662 (m), 600 (m), 659 (m), 575 (w), 572 (w), 500 (w), 448 (w). 1H NMR (600 MHz, 298 K, C_6D_5Br): $\delta = 7.32$ – 7.27 (m, 1H, C^4H of NPyr overlapping with bromobenzene signal), 7.22 (m, 2H, *m* of NPh), 7.07– 7.01 (m, 2H, *p* of NPh and C^6H of NPyr overlapping with bromobenzene signal), 6.61 (m, 1H, C^3H of NPyr), 6.40– 6.36 (m, 3H, *o* of NPh and C^5H of NPyr), 6.11 (s, 10H, Cp). $^{13}C\{^1H\}$ NMR (151 MHz, 298 K, C_6D_5Br): $\delta = 148.5$ (dm, $^1J_{CF} = 240$ Hz, *o* of C_6F_5), 146.5 (s, *i* of NPh), 145.7 (s, C^6H of NPyr), 144.6 (s, *i* of NPyr), 141.3 (C^4H of NPyr), 138.3 (dm, $^1J_{CF} = 240$ Hz, *p* of C_6F_5), 136.4 (dm, $^1J_{CF} = 240$ Hz, *m* of C_6F_5), 130.2 (s, *m* of NPh), 125.0 (s, *p* of NPh), 124.1 (bs, BC), 122.6 (s, Cp), 120.0 (s, *o* of NPh), 114.1 (s, C^5H of NPyr), 107.1 (s, C^3H of NPyr). $^{11}B\{^1H\}$ NMR (194 MHz, 298 K, C_6D_5Br): $\delta = -16.1$. $^{19}F\{^1H\}$ NMR (565 MHz, 298 K, C_6D_5Br): $\delta = -131.7$ (br s, 8F, *o* of C_6F_5), –161.7 (m, 4F, *p* of C_6F_5), –165.6 (br s, 8F, *m* of C_6F_5).

Irradiation Experiments. EPR samples of **1a–d** in a toluene/THF mixture were recorded before and after a 10s irradiation with an 18W LED lamp (**1a**: 405 nm; **1b**: 450 nm; **1c**: 405 nm; **1d**: 450 nm, 365 nm). In each case (except for **1d**), the previously reported cation $Cp_2Ti(THF)_2^+$ was observed.⁸ Additionally, for **1d**, a longer experiment was conducted: a THF- d_8 solution of **1d** was placed in a crimp-seal vial and irradiated in a photoreactor (18W, 450 nm) for 2 h. In this case, the $Cp_2Ti(THF)_2^+$ cation was observed.

Phenylsilane Polymerization. In an Ar glovebox the catalyst (0.04 mmol, 0.25 mol %) was weighed into a 250 mL Schlenk flask containing a large cross stir bar. The Schlenk was closed with a rubber septum and wrapped in aluminum foil to protect the complex from light. The phenylsilane (2 mL, 1.76 g, 16.3 mmol) was withdrawn into a syringe and removed from the glovebox. Outside of the glovebox, Schlenk was immersed into an oil bath set to 30 °C, stirring at 600 rpm, and attached to a vacuum/argon line. The reaction was connected to an open bubbler at all times and high flow of inert gas through the bubbler was established during the first 5 min of the reaction after which the flow was decreased to allow for gentle bubbling. Then the silane was added through the septum. An immediate and vigorous gas evolution was observed. **Caution!** A toxic and pyrophoric mixture of silane gas (SiH_4) and hydrogen (H_2) is produced which may ignite upon contact with air; a high flow of inert gas through the bubbler is necessary! The reaction mixture was stirred for 24 h. Before quenching the reaction was quickly evacuated and backfilled with argon 3 times to remove any residual silane gas. In the last cycle the Schlenk was backfilled with air and the viscous oily product was dissolved in 2 mL of toluene. The solution in toluene was added dropwise to 100 mL of vigorously stirred pentane, and a solid precipitated. The solid was filtered on a grade 4 frit, washed with 25 mL of pentane and dried under reduced pressure to give the polymer fraction. The pentane fraction was evaporated and the residue was subjected to Kugelrohr distillation (120 °C, 1–3 mbar) to give the diphenylsilane and the nonvolatile residue.

Hydrosilylation. A stock solution of catalyst in C_6H_5Br or C_6H_6 (≥ 9.2 mg) was prepared in an Ar glovebox. An aliquot (≥ 0.1 mL) was taken immediately and further diluted (total volume = 1 mL) to reach

the desired concentration. The silane (variable amount) and the reactant (1.0 mmol, 1 equiv) were added to the catalyst solution in a crimp-seal vial. The vials were sealed, and the reaction mixtures were stirred for the desired amount of time in a dry block heater outside of the glovebox. At the end of the reaction, the vials were opened to air, a 0.11 M solution of mesitylene in C_6D_6 (internal standard) was added, and the reaction mixtures were analyzed by 1H NMR spectroscopy at 500 MHz (298 K, 1 scan, 60s relaxation delay) and GCMS after further dilution with C_6D_6 and CH_2Cl_2 , respectively. All reactions were run in duplicate.

Stoichiometric Reactivity of 1Ia. Reaction of **1Ia** with Et_3SiH : In an Ar glovebox, complex **1Ia** (20.0 mg, 0.022 mmol) and Et_3SiH (11.5 mg, 0.099 mmol) were mixed in C_6D_5Br . The reaction mixture was analyzed by NMR spectroscopy, then PhCHO (11.6 mg, 0.109 mmol) was added and the mixture was analyzed again.

Reaction of **1Ia** with anisole, then Et_3SiH : In an Ar glovebox a stock solution of anisole in C_6D_5Br was prepared (11.7 mg/mL, 0.11 M). Complex **1Ia** (10 mg, 0.011 mmol) was dissolved in 0.5 mL of C_6D_5Br and the stock solution (0.1 mL, 0.011 mmol, 1.0 equiv) was added by syringe. The reaction mixture was transferred into a J. Young NMR tube, and the 1H NMR spectrum was acquired after 15 and 150 min.

The NMR tube was brought back into the glovebox and a solution of triethylsilane in deuterated bromobenzene (0.1 mL, 0.33 M, 0.033 mmol, 3.0 equiv) was added. The 1H NMR spectrum was measured 15 min after addition.

■ ASSOCIATED CONTENT

Supporting Information

The Supporting Information is available free of charge at <https://pubs.acs.org/doi/10.1021/acs.organomet.2c00642>.

Full experimental details and analyses for compounds **1a–d**, polymerization experiments and catalytic hydrosilylation runs (PDF)

Accession Codes

CCDC 2221753 contains the supplementary crystallographic data for this paper. These data can be obtained free of charge via www.ccdc.cam.ac.uk/data_request/cif, or by emailing data_request@ccdc.cam.ac.uk, or by contacting The Cambridge Crystallographic Data Centre, 12 Union Road, Cambridge CB2 1EZ, UK; fax: +44 1223 336033.

■ AUTHOR INFORMATION

Corresponding Authors

Adrien T. Normand – Institut de Chimie Moléculaire de L'Université de Bourgogne (ICMUB), Université de Bourgogne, Dijon 21000, France; orcid.org/0000-0002-8047-9386; Email: adrien.normand@u-bourgogne.fr

Pierre Le Gendre – Institut de Chimie Moléculaire de L'Université de Bourgogne (ICMUB), Université de Bourgogne, Dijon 21000, France; orcid.org/0000-0003-2635-5216; Email: pierre.le-gendre@u-bourgogne.fr

Authors

Tereza Edlová – Institut de Chimie Moléculaire de L'Université de Bourgogne (ICMUB), Université de Bourgogne, Dijon 21000, France

Hélène Cattey – Institut de Chimie Moléculaire de L'Université de Bourgogne (ICMUB), Université de Bourgogne, Dijon 21000, France

Stéphane Brandès – Institut de Chimie Moléculaire de L'Université de Bourgogne (ICMUB), Université de Bourgogne, Dijon 21000, France; orcid.org/0000-0001-6923-1630

Yue Wu – Department of Chemistry, Faculty of Science and Engineering, Swansea University, Swansea, Wales SA2 8PP, United Kingdom

Ariana Antonangelo – Department of Chemistry, Faculty of Science and Engineering, Swansea University, Swansea, Wales SA2 8PP, United Kingdom; orcid.org/0000-0002-1522-1338

Benjamin Théron – Institut de Chimie Moléculaire de L'Université de Bourgogne (ICMUB), Université de Bourgogne, Dijon 21000, France

Quentin Bonnin – Institut de Chimie Moléculaire de L'Université de Bourgogne (ICMUB), Université de Bourgogne, Dijon 21000, France

Mariolino Carta – Department of Chemistry, Faculty of Science and Engineering, Swansea University, Swansea, Wales SA2 8PP, United Kingdom; orcid.org/0000-0003-0718-6971

Complete contact information is available at:

<https://pubs.acs.org/10.1021/acs.organomet.2c00642>

Notes

The authors declare no competing financial interest.

ACKNOWLEDGMENTS

This paper is dedicated to Prof Gerhard Erker, in recognition of his outstanding contribution to the field of Group 4 chemistry. We are deeply indebted to Prof Ewen Bodio and Dr Christine Goze for sharing their financial resources. We thank Prof Anthony Romieu for the loan of a 365 nm LED lamp. We also thank Ms Tiffanie Regnier (PACSMUB) for elemental analyses. Financial support from CNRS, UB, Conseil Regional de Bourgogne Franche-Comte (PhosFerTiMn, PARI CDEA), and FEDER is gratefully acknowledged. Simulations of EPR spectra were performed using HPC resources from DSICCUB (Université de Bourgogne).

REFERENCES

- (1) Brintzinger, H. H.; Fischer, D.; Mülhaupt, R.; Rieger, B.; Waymouth, R. M. Stereospecific Olefin Polymerization with Chiral Metallocene Catalysts. *Angew. Chem., Int. Ed.* **1995**, *34*, 1143–1170.
- (2) Collins, R. A.; Russell, A. F.; Mountford, P. Group 4 metal complexes for homogeneous olefin polymerisation: a short tutorial review. *Applied Petrochemical Research* **2015**, *5*, 153–171.
- (3) Bochmann, M. The Chemistry of Catalyst Activation: The Case of Group 4 Polymerization Catalysts. *Organometallics* **2010**, *29*, 4711–4740.
- (4) Chen, E. Y.-X.; Marks, T. J. Cocatalysts for Metal-Catalyzed Olefin Polymerization: Activators, Activation Processes, and Structure–Activity Relationships. *Chem. Rev.* **2000**, *100*, 1391–1434.
- (5) Normand, A. T.; Daniliuc, C. G.; Wibbeling, B.; Kehr, G.; Le Gendre, P.; Erker, G. Phosphido- and Amidozirconocene Cation-Based Frustrated Lewis Pair Chemistry. *J. Am. Chem. Soc.* **2015**, *137*, 10796–10808.
- (6) Normand, A. T.; Daniliuc, C. G.; Kehr, G.; Le Gendre, P.; Erker, G. Direct P-functionalization of azobenzene by a cationic phosphidozirconocene complex. *Dalton Trans.* **2016**, *45*, 3711–3714.
- (7) Normand, A. T.; Daniliuc, C. G.; Wibbeling, B.; Kehr, G.; Le Gendre, P.; Erker, G. Insertion Reactions of Neutral Phosphidozirconocene Complexes as a Convenient Entry into Frustrated Lewis Pair Territory. *Chem. - Eur. J.* **2016**, *22*, 4285–4293.
- (8) Normand, A. T.; Bonnin, Q.; Brandès, S.; Richard, P.; Fleurat-Lessard, P.; Devillers, C. H.; Balan, C.; Le Gendre, P.; Kehr, G.; Erker, G. The Taming of Redox-Labile Phosphidotitanocene Cations. *Chem. - Eur. J.* **2019**, *25*, 2803–2815.
- (9) Bonnin, Q.; Edlová, T.; Sosa Carrizo, E. D.; Fleurat-Lessard, P.; Brandès, S.; Cattey, H.; Richard, P.; Le Gendre, P.; Normand, A. T. Coordinatively Unsaturated Amidotitanocene Cations with Inverted σ and π Bond Strengths: Controlled Release of Aminyl Radicals and Hydrogenation/Dehydrogenation Catalysis. *Chem. - Eur. J.* **2021**, *27*, 18175–18187.
- (10) See ref 5. Cationic Zr hydrides related to Cp_2ZrH^+ have been characterized by Jordan and are invoked as the active catalyst in the asymmetric hydrogenation of trisubstituted alkenes by Buchwald; see (a) Jordan, R. F.; Bajgur, C. S.; Dasher, W. E.; Rheingold, A. L. Hydrogenation of cationic dicyclopentadienylzirconium(IV) alkyl complexes. Characterization of cationic zirconium(IV) hydrides. *Organometallics* **1987**, *6*, 1041–1051. (b) Troutman, M. V.; Appella, D. H.; Buchwald, S. L. Asymmetric Hydrogenation of Unfunctionalized Tetrasubstituted Olefins with a Cationic Zirconocene Catalyst. *J. Am. Chem. Soc.* **1999**, *121*, 4916–4917.
- (11) Liu, H. Q.; Harrod, J. F. Dehydrocoupling of ammonia and silanes catalyzed by dimethyltitanocene. *Organometallics* **1992**, *11*, 822–827.
- (12) Shu, R.; Hao, L.; Harrod, J. F.; Woo, H.-G.; Samuel, E. Heterodehydrocoupling of Phosphines and Silanes Catalyzed by Titanocene: A Novel Route to the Formation of Si–P Bonds. *J. Am. Chem. Soc.* **1998**, *120*, 12988–12989.
- (13) Clark, T. J.; Russell, C. A.; Manners, I. Homogeneous, Titanocene-Catalyzed Dehydrocoupling of Amine–Borane Adducts. *J. Am. Chem. Soc.* **2006**, *128*, 9582–9583.
- (14) Helten, H.; Dutta, B.; Vance, J. R.; Sloan, M. E.; Haddow, M. F.; Sproules, S.; Collison, D.; Whittell, G. R.; Lloyd-Jones, G. C.; Manners, I. Paramagnetic Titanium(III) and Zirconium(III) Metallocene Complexes as Precatalysts for the Dehydrocoupling/Dehydrogenation of Amine–Boranes. *Angew. Chem., Int. Ed.* **2013**, *52*, 437–440.
- (15) LaPierre, E. A.; Patrick, B. O.; Manners, I. Trivalent Titanocene Alkyls and Hydrides as Well-Defined, Highly Active, and Broad Scope Precatalysts for Dehydropolymerization of Amine–Boranes. *J. Am. Chem. Soc.* **2019**, *141*, 20009–20015.
- (16) Berk, S. C.; Kreutzer, K. A.; Buchwald, S. L. A catalytic method for the reduction of esters to alcohols. *J. Am. Chem. Soc.* **1991**, *113*, 5093–5095.
- (17) Barr, K. J.; Berk, S. C.; Buchwald, S. L. Titanocene-Catalyzed Reduction of Esters Using Polymethylhydrosiloxane as the Stoichiometric Reductant. *J. Org. Chem.* **1994**, *59*, 4323–4326.
- (18) Verdager, X.; Lange, U. E. W.; Reding, M. T.; Buchwald, S. L. Highly Enantioselective Imine Hydrosilylation Using (*S,S*)-Ethylenebis(η^5 -tetrahydroindenyl)titanium Difluoride. *J. Am. Chem. Soc.* **1996**, *118*, 6784–6785.
- (19) Verdager, X.; Lange, U. E. W.; Buchwald, S. L. Amine Additives Greatly Expand the Scope of Asymmetric Hydrosilylation of Imines. *Angew. Chem., Int. Ed.* **1998**, *37*, 1103–1107.
- (20) Han, B.; Ren, C.; Jiang, M.; Wu, L. Titanium-Catalyzed Exhaustive Reduction of Oxo-Chemicals. *Angew. Chem., Int. Ed.* **2022**, *61*, e202209232.
- (21) Willoughby, C. A.; Buchwald, S. L. Asymmetric titanocene-catalyzed hydrogenation of imines. *J. Am. Chem. Soc.* **1992**, *114*, 7562–7564.
- (22) Willoughby, C. A.; Buchwald, S. L. Catalytic Asymmetric Hydrogenation of Imines with a Chiral Titanocene Catalyst: Kinetic and Mechanistic Investigations. *J. Am. Chem. Soc.* **1994**, *116*, 11703–11714.
- (23) Bareille, L.; Le Gendre, P.; Moise, C. First catalytic allyltitanation reactions. *Chem. Commun.* **2005**, 775–777.
- (24) Henriques, D. S. G.; Rojo-Wiechel, E.; Klare, S.; Mika, R.; Höthker, S.; Schacht, J. H.; Schmickler, N.; Gansäuer, A. Titanocene-(III)-Catalyzed Precision Deuteration of Epoxides. *Angew. Chem., Int. Ed.* **2022**, *61*, e202114198.
- (25) Selvakumar, K.; Harrod, J. F. Titanocene-Catalyzed Coupling of Amides in the Presence of Organosilanes To Form Vicinal Diamines. *Angew. Chem., Int. Ed.* **2001**, *40*, 2129–2131.

- (26) Rodriguez-Ruiz, V.; Carlino, R.; Bezzene-Lafollee, S.; Gil, R.; Prim, D.; Schulz, E.; Hannedouche, J. Recent developments in alkene hydro-functionalisation promoted by homogeneous catalysts based on earth abundant elements: formation of C-N, C-O and C-P bond. *Dalton Trans.* **2015**, *44*, 12029–12059.
- (27) Davis-Gilbert, Z. W.; Tonks, I. A. Titanium redox catalysis: insights and applications of an earth-abundant base metal. *Dalton Trans.* **2017**, *46*, 11522–11528.
- (28) Reed-Berendt, B. G.; Polidano, K.; Morrill, L. C. Recent advances in homogeneous borrowing hydrogen catalysis using earth-abundant first row transition metals. *Org. Biomol. Chem.* **2019**, *17*, 1595–1607.
- (29) Bullock, R. M.; Chen, J. G.; Gagliardi, L.; Chirik, P. J.; Farha, O. K.; Hendon, C. H.; Jones, C. W.; Keith, J. A.; Klosin, J.; Minter, S. D.; Morris, R. H.; Radosevich, A. T.; Rauchfuss, T. B.; Strotman, N. A.; Vojvodic, A.; Ward, T. R.; Yang, J. Y.; Surendranath, Y. Using nature's blueprint to expand catalysis with Earth-abundant metals. *Science* **2020**, *369*, eabc3183.
- (30) Wailes, P. C.; Weigold, H. Hydrido complexes of zirconium I. Preparation. *J. Organomet. Chem.* **1970**, *24*, 405–411.
- (31) Hart, D. W.; Schwartz, J. Hydrozirconation. Organic synthesis via organozirconium intermediates. Synthesis and rearrangement of alkylzirconium(IV) complexes and their reaction with electrophiles. *J. Am. Chem. Soc.* **1974**, *96*, 8115–8116.
- (32) Wipf, P.; Kendall, C. Hydrozirconation and Its Applications. *Top. Organomet. Chem.* **2004**, *8*, 1–25.
- (33) Lipschutz, B. H.; Pfeiffer, S. S.; Noson, K.; Tomioka, T. Hydrozirconation and Further Transmetalation Reactions. In *Titanium and Zirconium in Organic Synthesis*; Marek, I., Ed.; Wiley-VCH, 2002; pp 110–148.
- (34) Kobylarski, M.; Donnelly, L. J.; Berthet, J.-C.; Cantat, T. Zirconium-catalysed hydrosilylation of esters and depolymerisation of polyester plastic waste. *Green Chem.* **2022**, *24*, 6810–6815.
- (35) Donnelly, L. J.; Berthet, J.-C.; Cantat, T. Selective Reduction of Secondary Amides to Imines Catalysed by Schwartz's Reagent. *Angew. Chem., Int. Ed.* **2022**, *61*, e202206170.
- (36) Lauher, J. W.; Hoffmann, R. Structure and chemistry of bis(cyclopentadienyl)-ML_n complexes. *J. Am. Chem. Soc.* **1976**, *98*, 1729–1742.
- (37) Due to i) their high sensitivity towards air and moisture; ii) their propensity to form clathrates with the solvent used for workup (pentane); and iii) their high fluorine content, satisfactory elemental analyses could not be obtained despite repeated attempts. We report the "least worst" result for each compound, however statistically insignificant. For a recent discussion on the relevance of publishing single point elemental analysis results, see Kuvke, R. E. H.; Barwise, L.; van Ingen, Y.; Vashisth, K.; Roberts, N.; Chitnis, S. S.; Dutton, J. L.; Martin, C. D.; Melen, R. L. An International Study Evaluating Elemental Analysis. *ACS Central Science* **2022**, *8*, 855–863.
- (38) Halbert, S.; Copéret, C.; Raynaud, C.; Eisenstein, O. Elucidating the Link between NMR Chemical Shifts and Electronic Structure in d⁰ Olefin Metathesis Catalysts. *J. Am. Chem. Soc.* **2016**, *138*, 2261–2272.
- (39) Juliá, F. Ligand-to-Metal Charge Transfer (LMCT) Photochemistry at 3d-Metal Complexes: An Emerging Tool for Sustainable Organic Synthesis. *ChemCatChem* **2022**, *14*, e202200916.
- (40) Breslow, D. S.; Newburg, N. R. Bis-(cyclopentadienyl)-Titanium Dichloride-Alkylaluminum Complexes as Catalysts for the Polymerization of Ethylene. *J. Am. Chem. Soc.* **1957**, *79*, 5072–5073.
- (41) Breslow, D. S.; Newburg, N. R. Bis-(cyclopentadienyl)-titanium Dichloride-Alkylaluminum Complexes as Soluble Catalysts for the Polymerization of Ethylene. *J. Am. Chem. Soc.* **1959**, *81*, 81–86.
- (42) RajanBabu, T. V.; Nugent, W. A. Selective Generation of Free Radicals from Epoxides Using a Transition-Metal Radical. A Powerful New Tool for Organic Synthesis. *J. Am. Chem. Soc.* **1994**, *116*, 986–997.
- (43) Li, J.-N.; Liu, L.; Fu, Y.; Guo, Q.-X. What are the pK_a values of organophosphorus compounds? *Tetrahedron* **2006**, *62*, 4453–4462.
- (44) The case of **1c** is different, in that the observed species do(es) not appear to contain nitrogen.
- (45) Neugebauer, F. A.; Fischer, P. H. H. Zur Dissoziation der Tetraarylhidrazine. *Chem. Ber.* **1965**, *98*, 844–850.
- (46) Neugebauer, F. A.; Bamberger, S. Diphenylaminyl. *Angew. Chem., Int. Ed.* **1971**, *10*, 71.
- (47) Oberdorf, K.; Hanft, A.; Ramler, J.; Krummenacher, I.; Bickelhaupt, F. M.; Poater, J.; Lichtenberg, C. Bismuth Amides Mediate Facile and Highly Selective Pn–Pn Radical-Coupling Reactions (Pn = N, P, As). *Angew. Chem., Int. Ed.* **2021**, *60*, 6441–6445.
- (48) Aitken, C.; Harrod, J. F.; Samuel, E. Polymerization of primary silanes to linear polysilanes catalyzed by titanocene derivatives. *J. Organomet. Chem.* **1985**, *279*, C11–C13.
- (49) Aitken, C. T.; Harrod, J. F.; Samuel, E. Identification of some intermediates in the titanocene-catalyzed dehydrogenative coupling of primary organosilanes. *J. Am. Chem. Soc.* **1986**, *108*, 4059–4066.
- (50) Gauvin, F.; Harrod, J. F. Evidence for stereoregulations in the polymerisation of phenylsilane by bis (indenyl)dimethylzirconium complexes. *Can. J. Chem.* **1990**, *68*, 1638–1640.
- (51) Li, H.; Gauvin, F.; Harrod, J. F. Observations concerning the inactivity of dimethylhafnocene as a catalyst for the dehydrocoupling of phenylsilane. *Organometallics* **1993**, *12*, 575–577.
- (52) Dioumaev, V. K.; Harrod, J. F. Catalytic Dehydrocoupling of Phenylsilane with "Cation-like" Zirconocene Derivatives: A New Approach to Longer Silicon Chains. *Organometallics* **1994**, *13*, 1548–1550.
- (53) Dioumaev, V. K.; Harrod, J. F. A systematic analysis of the structure-reactivity trends for some 'cation-like' early transition metal catalysts for dehydropolymerization of silanes. *J. Organomet. Chem.* **1996**, *521*, 133–143.
- (54) Gauvin, F.; Harrod, J. F.; Woo, H. G. Catalytic Dehydrocoupling: A General Strategy for the Formation of Element–Element Bonds. *Adv. Organomet. Chem.* **1998**, *42*, 363–405.
- (55) Dioumaev, V. K.; Rahimian, K.; Gauvin, F.; Harrod, J. F. Stereostructures of Linear and Cyclic Polyphenylsilanes Produced by Dehydrocoupling in the Presence of Group 4 Metallocene Catalysts. *Organometallics* **1999**, *18*, 2249–2255.
- (56) Harrod, J. F. Catalysis of reactions of Si–H by titanocene and its derivatives. *Coord. Chem. Rev.* **2000**, *206–207*, 493–531.
- (57) Woo, H. G.; Walzer, J. F.; Tilley, T. D. σ -Bond metathesis mechanism for dehydropolymerization of silanes to polysilanes by d⁰ metal catalysts. *J. Am. Chem. Soc.* **1992**, *114*, 7047–7055.
- (58) Tilley, T. D. The coordination polymerization of silanes to polysilanes by a " σ -bond metathesis" mechanism. Implications for linear chain growth. *Acc. Chem. Res.* **1993**, *26*, 22–29.
- (59) Imori, T.; Tilley, T. D. The influence of catalyst structure on the dehydropolymerization of phenylsilane. *Polyhedron* **1994**, *13*, 2231–2243.
- (60) Bourg, S.; Corriu, R. J. P.; Enders, M.; Moreau, J. J. E. New Stable Titanocene and Zirconocene Catalyst Precursors for Polysilane Synthesis via Dehydrocoupling of Hydrosilanes. *Organometallics* **1995**, *14*, 564–566.
- (61) Grimmond, B. J.; Corey, J. Y. Catalytic Dehydropolymerization of PhSiH₃ to Polyphenylsilane with Substituted Group IV Metallocenes. *Organometallics* **1999**, *18*, 2223–2229.
- (62) Grimmond, B. J.; Corey, J. Y. Synthesis and Characterization of Atactic Poly(p-tolylsilane) via the Catalytic Dehydrocoupling of p-Tolylsilane. *Organometallics* **2000**, *19*, 3776–3783.
- (63) Grimmond, B. J.; Corey, J. Y. Amino-functionalized zirconocene (C₅H₄CH(Me)NMe₂)₂ZrCl₂, a catalyst for the dehydropolymerization of PhSiH₃: Probing of peripheral substituent effects on catalyst dehydropolymerization activity. *Inorg. Chim. Act.* **2002**, *330*, 89–94.
- (64) Miller, R. D.; Michl, J. Polysilane high polymers. *Chem. Rev.* **1989**, *89*, 1359–1410.
- (65) Chauhan, N. P. S. Polysilanes and Other Silicon-Containing Polymers. In *Inorganic and Organometallic Polymers*; Springer Berlin Heidelberg: Berlin, Heidelberg, 2005; pp 249–295.

- (66) Feigl, A.; Bockholt, A.; Weis, J.; Rieger, B. Modern Synthetic and Application Aspects of Polysilanes: An Underestimated Class of Materials? In *Silicon Polymers*; Muzafarov, A. M., Ed.; Springer Berlin Heidelberg: Berlin, Heidelberg, 2011; pp 1–31.
- (67) Koe, J.; Fujiki, M. Chapter 6 - Polysilanes. In *Organosilicon Compounds*; Lee, V. Y., Ed.; Academic Press: 2017; pp 219–300.
- (68) Kumar, V. B.; Leitao, E. M. Properties and applications of polysilanes. *Appl. Organomet. Chem.* **2020**, *34*, e5402.
- (69) These are also observed with catalysts based on other transition metals (e.g., Mo, Ni, Ir). See (a) Minato, M.; Matsumoto, T.; Ichikawa, M.; Ito, T. Dehydropolymerization of arylsilanes catalyzed by a novel silylmolybdenum complex. *Chem. Commun.* **2003**, 2968–2969. (b) Tanabe, M.; Takahashi, A.; Fukuta, T.; Osakada, K. Nickel-Catalyzed Cyclopolymerization of Hexyl- and Phenylsilanes. *Organometallics* **2013**, *32*, 1037–1043. Smith, E. E.; Du, G.; Fanwick, P. E.; Abu-Omar, M. M. Dehydrocoupling of Organosilanes with a Dinuclear Nickel Hydride Catalyst and Isolation of a Nickel Silyl Complex. *Organometallics* **2010**, *29*, 6527–6533. (d) Mucha, N. T.; Waterman, R. Iridium Pincer Catalysts for Silane Dehydrocoupling: Ligand Effects on Selectivity and Activity. *Organometallics* **2015**, *34*, 3865–3872.
- (70) Dioumaev, V. K.; Harrod, J. F. Studies of the Formation and Decomposition Pathways for Cationic Zirconocene Hydrido Silyl Complexes. *Organometallics* **1997**, *16*, 2798–2807.
- (71) Waterman, R. Mechanisms of metal-catalyzed dehydrocoupling reactions. *Chem. Soc. Rev.* **2013**, *42*, 5629–5641.
- (72) Söllradl, H.; Hengge, E. Vergleichende ^{29}Si -NMR-untersuchungen an verschiedenen disilanderivaten. *J. Organomet. Chem.* **1983**, *243*, 257–269.
- (73) Mucha, N. T.; Waterman, R. Iridium Pincer Catalysts for Silane Dehydrocoupling: Ligand Effects on Selectivity and Activity. *Organometallics* **2015**, *34*, 3865–3872.
- (74) No cyclic oligomers were observed in the liquid fraction; see [Figure S47](#).
- (75) The MALDI-TOF spectrum was uninformative; see [Figure S54](#).
- (76) Lee, P. T. K.; Rosenberg, L. Borane-catalysed postpolymerisation modification of the Si–H bonds in poly(phenylsilane). *Dalton Trans.* **2017**, *46*, 8818–8826.
- (77) We base our assignments on data from the literature.^{73,76,78,79} Broad signals are to be expected for polyphenylsilane samples obtained by dehydrocoupling; see for example [Figure 3](#) in [ref 76](#). Overall, there is a consensus in the literature regarding the location of PhSiH – signals (by ^1H NMR spectroscopy as well as ^{29}Si DEPT) in cyclic oligomers, as well as Ph_2SiH – signals in linear polymers. In our case, we observe additional signals corresponding to Ph_2SiH – end caps, but this has been observed in the past by Waterman (see page 3869 in [ref 73](#)); we also observe broad resonances at high field which we assign to SiH – branch points by analogy to compounds E and M (table XII in [ref 79](#)).
- (78) Feigl, A.; Chiorescu, I.; Deller, K.; Heidsieck, S. U. H.; Buchner, M. R.; Karttunen, V.; Bockholt, A.; Genest, A.; Rösch, N.; Rieger, B. Metal-Free Polymerization of Phenylsilane: Tris(pentafluorophenyl)-borane-Catalyzed Synthesis of Branched Polysilanes at Elevated Temperatures. *Chem. - Eur. J.* **2013**, *19*, 12526–12536.
- (79) Hahn, J. Beiträge zur Chemie des Siliciums und Germaniums, XXIX [1] ^{29}Si -NMR-spektroskopische Untersuchungen von geradkettigen und verzweigten Silanen. *Z. Naturforsch. B* **1980**, *35*, 282–296.
- (80) Berk, S. C.; Buchwald, S. L. An air-stable catalyst system for the conversion of esters to alcohols. *J. Org. Chem.* **1992**, *57*, 3751–3753.
- (81) Reding, M. T.; Buchwald, S. L. An Inexpensive Air-Stable Titanium-Based System for the Conversion of Esters to Primary Alcohols. *J. Org. Chem.* **1995**, *60*, 7884–7890.
- (82) Hansen, M. C.; Buchwald, S. L. A Method for the Asymmetric Hydrosilylation of N-Aryl Imines. *Org. Lett.* **2000**, *2*, 713–715.
- (83) Yun, J.; Buchwald, S. L. Efficient Kinetic Resolution in the Asymmetric Hydrosilylation of Imines of 3-Substituted Indanones and 4-Substituted Tetralones. *J. Org. Chem.* **2000**, *65*, 767–774.
- (84) Willoughby, C. A.; Buchwald, S. L. Synthesis of highly enantiomerically enriched cyclic amines by the catalytic asymmetric hydrogenation of cyclic imines. *J. Org. Chem.* **1993**, *58*, 7627–7629.
- (85) Kehner, R. A.; Hewitt, M. C.; Bayeh-Romero, L. Expanding Zirconocene Hydride Catalysis: In Situ Generation and Turnover of ZrH Catalysts Enabling Catalytic Carbonyl Reductions. *ACS Catal.* **2022**, *12*, 1758–1763.
- (86) Miyai, T.; Onishi, Y.; Baba, A. Indium trichloride catalyzed reductive Friedel-Crafts alkylation of aromatics using carbonyl compounds. *Tetrahedron Lett.* **1998**, *39*, 6291–6294.
- (87) Saito, S.; Ohwada, T.; Shudo, K. Friedel-Crafts-type reaction of benzaldehyde with benzene. Diprotonated benzaldehyde as the reactive intermediate. *J. Am. Chem. Soc.* **1995**, *117*, 11081–11084.
- (88) For a similar reaction catalyzed by $\text{B}(\text{C}_6\text{F}_5)_3$, see Bézier, D.; Park, S.; Brookhart, M. Selective Reduction of Carboxylic Acids to Aldehydes Catalyzed by $\text{B}(\text{C}_6\text{F}_5)_3$. *Org. Lett.* **2013**, *15*, 496–499.
- (89) Since only $(\text{Et}_3\text{Si})_2\text{O}$ was observed in the reaction of methyl benzoate (entry 10, [Figures S73 and S74](#)), whereas MeOSiEt_3 could be observed when Zr was used as a catalyst (entries 8 and 9, [Figures S69–S72](#)), we surmise that, in the case of Ti, MeOSiEt_3 is deoxygenated further to yield CH_4 and $(\text{Et}_3\text{Si})_2\text{O}$. This is consistent with the tendency for complete reduction of the Ti catalyst on the one hand, and the observed pressure buildup, which is also due to the release of H_2 due to the Friedel–Crafts reaction, on the other hand.
- (90) Torrens, A. A.; Ly, A. L.; Fong, D.; Adronov, A. Rapid and Mild Cleavage of Aryl-Alkyl Ethers to Liberate Phenols. *Eur. J. Org. Chem.* **2022**, *2022*, e202200570.
- (91) Gevorgyan, V.; Rubin, M.; Benson, S.; Liu, J.-X.; Yamamoto, Y. A Novel $\text{B}(\text{C}_6\text{F}_5)_3$ -Catalyzed Reduction of Alcohols and Cleavage of Aryl and Alkyl Ethers with Hydrosilanes. *J. Org. Chem.* **2000**, *65*, 6179–6186.
- (92) Blackwell, J. M.; Foster, K. L.; Beck, V. H.; Piers, W. E. $\text{B}(\text{C}_6\text{F}_5)_3$ -Catalyzed Silylation of Alcohols: A Mild, General Method for Synthesis of Silyl Ethers. *J. Org. Chem.* **1999**, *64*, 4887–4892.
- (93) Petasis, N. A.; Morshed, M. M.; Ahmad, M. S.; Hossain, M. M.; Trippier, P. C., Eds. In *Encyclopedia of Reagents for Organic Synthesis*; John Wiley & Sons, Ltd.: Chichester, U.K., 2012.
- (94) Ihara, E.; Young, V. G., Jr.; Jordan, R. F., Jr. Cationic Aluminum Alkyl Complexes Incorporating Aminotroponimate Ligands. *J. Am. Chem. Soc.* **1998**, *120*, 8277–8278.
- (95) Zhang, H.; Cai, Q.; Ma, D. Amino Acid Promoted CuI-Catalyzed C–N Bond Formation between Aryl Halides and Amines or N-Containing Heterocycles. *J. Org. Chem.* **2005**, *70*, 5164–5173.
- (96) Lv, Z.; Liu, J.; Wei, W.; Wu, J.; Yu, W.; Chang, J. Iodine-Mediated Aryl C–H Amination for the Synthesis of Benzimidazoles and Pyrido[1,2-a]benzimidazoles. *Adv. Synth. Catal.* **2016**, *358*, 2759–2766.